
POWER MINIMIZATION OF DOWNLINK SPECTRUM SLICING FOR eMBB AND URLLC USERS

A PREPRINT

Fabio Saggese
Dept. of Information Engineering
University of Pisa
 Pisa, Italy
 fabio.saggese@phd.unipi.it

Marco Moretti
Dept. of Information Engineering
University of Pisa
 Pisa, Italy
 marco.moretti@unipi.it

Petar Popovski
Dept. of Electronic Systems
Aalborg University
 Aalborg, Denmark
 petarp@es.aau.dk

June 8, 2022

Abstract

5G technology allows the presence of heterogeneous services in the same physical network. On the radio access network (RAN), the *spectrum slicing* of the shared radio resources is a critical task to guarantee the performance of each service. In this paper, we analyze a downlink communication in which a base station (BS) should serve two types of traffic, enhanced mobile broadband (eMBB) and ultra-reliable low-latency communication (URLLC), respectively. Due to the nature of low-latency traffic, the BS knows the channel state information (CSI) of the eMBB users only. In this setting, we study the power minimization problem employing orthogonal multiple access (OMA) and non-orthogonal multiple access (NOMA) schemes. We analyze the impact of resource sharing, showing that the knowledge of eMBB CSI can be used also in resource allocation for URLLC users. Based on this analysis, we propose two algorithms: a feasible and a block coordinated descent approach (BCD). We show that the BCD is optimal for the URLLC power allocation. The numerical results show that NOMA leads to a lower power consumption compared to OMA, except when the URLLC user is very close to the BS. For the last case, the optimal approach depends on the channel condition of the eMBB user. In any case, even when the OMA paradigm attains the best performance, the gap with NOMA is negligible, proving the NOMA capacity in exploiting the shared resources to reduce the power consumption in every condition.

Keywords NOMA · RAN slicing · eMBB · URLLC · Power saving

1 Introduction

The whole plethora of new services that 5G and beyond technology promises to provide has brought the need to sustain very heterogeneous requirements in the same physical network. Some services will require very strict requirements in terms of latency, others high reliability, or a huge number of devices connected to the network, while the majority of “traditional” services will still require high bandwidth and data rate. To address the complexity of such a vast space of requirement, 5G standardized three generic service types: enhanced mobile broadband (eMBB), massive machine-type communications (mMTC), and ultra-reliable low-latency communications (URLLC) [1]. Note that these three generic definitions must not be seen as exclusive: a realistic service could require any combination of the aforementioned generic service types.

In this context, *spectrum slicing* will become a fundamental task in 5G and beyond Radio Access Network (RAN): how to allocate a given chunk of spectrum to serve users with heterogeneous requirements. This terminology is motivated by the more general concept of network slicing: partitioning the physical network infrastructure in different end-to-end isolated virtual networks able to support different service requirements for the various use cases [2]. In that sense, we can also refer to spectrum slicing as RAN slicing.

The general problem of resource allocation for RAN slicing has been firstly discussed in [3], where the authors allocate resource block (RB) to different base stations (BS) to meet the demand of mobile network operators. This prior work gave one of the first formalizations of the RAN slicing problem, even if it did not take into account the physical layer requirements. Several works treated the problem of resource allocation algorithms to multiplex eMBB and URLLC services. In [4], the joint resource allocation problem for eMBB-URLLC slicing is addressed employing different puncturing models, where the reliability of the URLLC transmission is always considered met. The authors of [5] and [6] propose two deep reinforcement learning techniques to allocate the resource to the two services, employing orthogonal resources and pre-emption/puncturing, respectively. The instantaneous channel state information (CSI) is a crucial parameter to let these algorithms properly work. The previous works consider the current 5G standard application of dynamic resources sharing between eMBB and URLLC, i.e., by means of puncturing or non-overlapping time/frequency resources [1]. However, NOMA has proven to outperform the OMA in many applications [7], as shown in the previous Chapters. Spectrum slicing can be realized by these two principal approaches, OMA and NOMA, as introduced in the uplink communication framework presented in [8]. The performance comparison between NOMA and OMA is also been investigated in [9] for URLLC devices with different latency requirements in the uplink direction. Furthermore, the performance of the OMA case with limited feedback by the receiver is presented. In [10], a reinforcement learning algorithm decides whenever to use OMA or NOMA for dynamic multiplexing of eMBB-URLLC data streams, setting the transmission power based on the information of the channel state. In [11] the use of OMA and NOMA in uplink direction for intermittent and broadband services are studied. The reliability is enforced by employing packet coding on binary erasure channel, while the latency is modeled taking into account reliability-latency and age of information metrics.

1.1 Contributions

In this paper, we analyze the spectrum slicing problem for downlink transmissions of eMBB and URLLC traffic. The resources available follow the 5G NR standard, assuming that the time coherence of the channels lasts enough to include an entire time-slot. The eMBB service aims to maximize the throughput while not having a latency requirement. On the contrary, the URLLC service demands mission-critical, reliable communication, where a hard latency constraint must be fulfilled. We aim to guarantee a reliable URLLC transmission while assuring a minimum spectral efficiency transmission toward the eMBB user. Considering the intermittent nature of URLLC and the stringent latency constraints, the estimation of CSI is infeasible, while possible for the eMBB device. Hence, we assume the knowledge of the statistical CSI of the URLLC user, while the instantaneous CSI for the eMBB user is available at the BS. In this setting, we investigate the minimization of power for the eMBB-URLLC spectrum slicing problem for both the NOMA and OMA downlink paradigms. Then, the comparison is made seeking the approach that leads to the lowest power consumption.

Here, we do not analyze explicitly the puncturing method, being an orthogonal transmission. Thus, using puncturing can be modeled as the OMA transmission depicted in the remainder of the paper. Moreover, to guarantee the performance required by the eMBB transmission, some protection mechanisms on the punctured resources must be performed, e.g., erasure [8], or packet-level codes [11]. These protection methods employ more power than strictly needed to add redundancy to the punctured data stream. However, this is clearly not an optimal approach for our setting, considering that we are interested in saving power by guaranteeing the traffic requirements. Therefore, we focus on OMA and NOMA allocation process, remarking that the same approach can be extended for puncturing.

Knowing only the statistical CSI, a common approach to satisfy the performance of a URLLC user is employing the outage probability, which depends on the number of resources selected, the spectral efficiency of the transmission, the mean signal-to-noise ratio at the receiver. However, the optimization of the resources and power allocation problem for the URLLC is a difficult task, taking into account that the closed form expression of the outage probability for a parallel channel environment can be obtained only in particular cases [12]. Even approximations of the outage probability as [13, 14] are not easy to be addressed in an optimization problem involving non-convex special functions. Moreover, the use of NOMA leads to an even more complex evaluation of outage probability, given by the interference channel [15, 16]. Therefore, even if the setting studied in this paper is simple, it requires complex analysis. On the other hand, the study made in this paper is, in fact, without loss of generalization if each set of resources is shared to a couple of users with heterogeneous traffic. The results provided help to understand the impact of pairing users on the overall power consumption of the transmission. The investigation of more than two users sharing the same

group of resources is a future step of this research. To the best of our knowledge, even this simple scenario has not been investigated with these assumptions.

We believe this study is a promising step to design a scheduler able to employ spectrum slicing on the physical layer. The contributions of this work are the following:

- Analyzing the heterogeneous requirements, we found that the knowledge of eMBB instantaneous CSI is beneficial also for the URLLC allocation. We show that the overall allocation problem can be split into simpler sub-problems. Then, the eMBB CSI is used to obtain the allocation strategy of the eMBB transmission, which is, in turn, used to properly select the resources for the URLLC transmission.
- We provide a closed form solution to guarantee the successive interference cancellation (SIC) for the downlink setting. Moreover, we also study the interference-limited scenario, i.e., when the interference is dominant w.r.t. the noise. We show experimentally that the noise is negligible if the URLLC channel conditions are better than the eMBB ones.
- Using the previous problem splitting procedure, we propose a feasible resource allocation, working for both OMA and NOMA paradigms. We further demonstrate that this algorithm provides an optimal allocation of URLLC resources when employed for the OMA paradigm.
- In order to compare the performance with the optimal solution, we also propose a BCD algorithm able to provide the optimal solution for the NOMA URLLC resource allocation.
- For the OMA paradigm, we provide different results for different reserved resources for the two traffic types. We show that different parameters lead to a diverse optimal solution for the OMA case. The number of orthogonal frequencies reserved affects the power consumption of the eMBB and URLLC data transmission. In general, more resources given to URLLC means a lower power needed to fulfill URLLC requirements, while the power guaranteeing the eMBB data rate increases and vice-versa. The optimal solution is obtained by finding a trade-off of these two effects.
- We show that the NOMA access paradigm outperforms the OMA for almost every parameter of interest. There are particular situations where the OMA performs slightly better; however, the performance in these situations is still comparable. This behavior is given by the fact that NOMA may allow the URLLC transmission to be made on top of scheduled eMBB resources without disrupting the eMBB data stream. Hence, we can share all the resources available to both users. In other words, we allow a certain degree of interference to exploit the higher frequency diversity gain, provided by the higher number of resources employed.
- The results show that the performance gap between feasible and BCD algorithms is generally negligible; hence, a very good solution can be found exploiting feasible and lower complexity approaches.

Paper outline The remainder of the paper is organized as follows. In section 2 the environment and the signal model are described. In the same Section, we focus also on the overall information transmittable and the possible outage events that may occur to the users. In Section 3, the allocation process is described. In particular, we firstly describe the minimization power problem; then, we describe how to split the problem to obtain a low-complexity feasible solution. In Section 4 we describe the two algorithms proposed. Results are presented in Section 5 and conclusions in Section 6.

Mathematical notation In the remainder of the paper, we use capital italic letter to represent sets, e.g. \mathcal{A} , while their cardinality is denoted with capital letter, e.g. A . We denote the operator $\mathcal{A} \setminus \mathcal{B} = \{x \in \mathcal{A}, x \notin \mathcal{B}\}$. Vector are presented in bold uppercase letters \mathbf{P} ; the symbol \succeq represent the element-wise comparison between vectors. We also denote with the symbol $\mathbf{1}$ the vector composed by ones everywhere, and the vector $\mathbf{0}$ composed by only zeros. The symbol $\mathcal{CN}(a, B)$ represents complex Gaussian distribution with mean value a and variance B , while $\text{Exp}(a)$ represents the exponential distribution with mean value a .

2 System Model

We study a 5G-like single-cell downlink scenario, where, to capture the nature of the dynamics of the slicing problem, we consider only two users: an eMBB user and a URLLC user. In the remainder of the paper, we will use the letters u to indicate the URLLC user and e to indicate the eMBB user.

The available resources are organized in a time-frequency grid. In the time domain we consider a single time-slot of duration T [s]. For low-latency communications, the time-slot is further divided into a set of

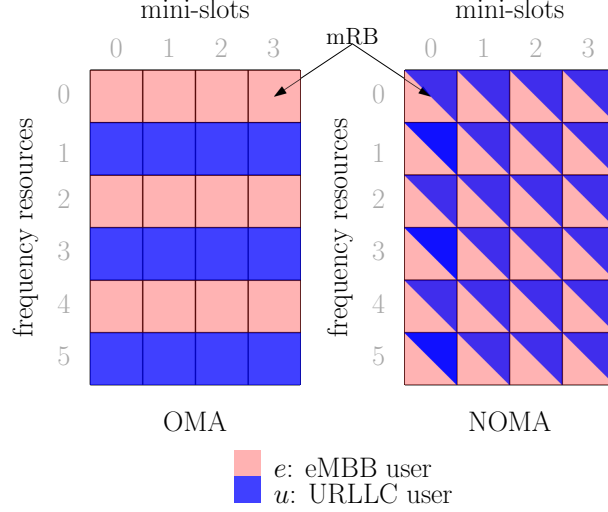


Figure 1: Toy example of resource allocation grid of $F = 6$, $M = 4$. In this example, we reserve the $F_u = 3$ resources for the OMA configuration, where $\mathcal{F}_u = \{1, 3, 5\}$. In the case of NOMA, the transmission is made onto the whole grid, i.e., $F_u = 5$. We will show that it is possible to guarantee the requirements of both users with this configuration.

mini-slots $\mathcal{M} = \{0, \dots, M - 1\}$, $|\mathcal{M}| = M$, each one of duration $T_m = T/M$ [s]. We assume that the coherence time of the channel T_c is $T_c \geq T$ so that the channel gains can be assumed constant during an entire time-slot. In the frequency domain, we consider a set $\mathcal{F} = \{0, \dots, F - 1\}$, $|\mathcal{F}| = F$ of orthogonal frequency resources, each occupying a bandwidth Δ_f [Hz]. In the remainder of the paper, we call a single time-frequency resource as a *mini resource block* (mRB), where the term “mini” is used to highlight the reduced dimension in time to a conventional resource block.

The two users have different objectives and constraints: the eMBB user is modeled as transmitting a pipeline of N_e informative bits per slot, while the URLLC user has to meet specific requirements in terms of latency and reliability. In detail, we assume that a packet containing N_u informative bits must be delivered within T_u seconds with an outage probability lower than ϵ_u . Latency constraints are expressed as a function of the *edge delay*, i.e. the delay between the time at which the message arrives at the transmitter and the time at which the message is effectively transmitted towards the user, assuming that all other delay terms have already subtracted from T_u [17]. Without loss of generality, the tolerable latency is expressed as a maximum number of mini-slots M_u^{\max} .

Resources are assigned to the users on the basis of their traffic type (URLLC or eMBB) and the multiple access technology adopted (OMA or NOMA). Following the 5G NR standard [1], the URLLC data transmission is allowed to span a certain number of mini-slots, due to the critical time communication. On the other hand, the resource allocation for eMBB transmission can only span the entire slot, in order to support a high communication rate. To formalize this concept, we denote as $\mathcal{F}_u \subseteq \mathcal{F}$, $|\mathcal{F}_u| = F_u$, and $\mathcal{M}_u \subseteq \mathcal{M}$, $|\mathcal{M}_u| = M_u$, the sets of frequency and temporal resources allocated for the *transmission* of the data stream of user u . It is worth noting that the URLLC tolerable latency constraints the transmission time $M_u \leq M$, while the F_u resources are reserved for the entire slot, i.e. for M mini-slots. In other words, if a subset of the mRBs is reserved for the URLLC, this reservation lasts for the whole time-slot. We remark that increasing the time duration of the URLLC data transmission will reduce the power needed to transmit the same amount of information. However, this increases also the latency a URLLC packet can experience if it arrives when the previous packet is still in transmission. To correctly compare the schemes, we assume that only a single URLLC packet has to be served. This assumption is without loss of generality if another packet arrives during the transmission is allocated on a different set of resources. The subset of the mRBs reserved for e is denoted as $\mathcal{F}_e \subseteq \mathcal{F}$, $|\mathcal{F}_e| = F_e$, while its set of temporal resources is denoted as $\mathcal{M}_e \subseteq \mathcal{M}$, $|\mathcal{M}_e| = M_e$. To support high data rate, we exploit all the available time for the transmission of eMBB data stream, resulting in $\mathcal{M}_e = \mathcal{M}$. The frequency allocation depends on the multiple access scheme employed. In the case of OMA, this means that the each mRB reserved for u cannot be given to e for specific mini-slots. In the case of NOMA, this means that all the resources reserved for e are shared with u , as soon as the u

transmission will not disrupt the eMBB requirements. Hence, the set \mathcal{F}_e results

$$\mathcal{F}_e = \begin{cases} \mathcal{F} \setminus \mathcal{F}_u, & \text{OMA,} \\ \mathcal{F}, & \text{NOMA.} \end{cases} \quad (1)$$

An example of the resource allocation grid for both OMA and NOMA is presented in Fig. 1.

Given the number of resources assigned to user $i \in \{e, u\}$, and N_i , the number of informative bits to be transmitted for user i , the average spectral efficiency per resource is obtained as

$$r_i = \frac{N_i}{T_m \Delta_f F_i M_i} \quad [\text{bit/s/Hz}] \quad i \in \{e, u\}. \quad (2)$$

Finally, the transmitter possesses different knowledge of the channel gains of the two different types of traffic. Instantaneous CSI is not available at the transmitter for URLLC traffic due to the time-critical nature of this service, and thus we assume that only the mean signal-to-noise ratio (SNR) Γ_u , accounting for both large-scale fading and noise at the receiver, is known. On the other hand, we assume the complete knowledge of the instantaneous CSI for the eMBB user.

It is worth noting that the same model can be used when the URLLC transmission is made through puncturing of the eMBB data. In that case, the number of mRBs given to URLLC is always $F_u = F$. To fulfill the eMBB decoding requirement expecting m punctured mini-slots, the eMBB resource allocation must be made presuming that the mini-slots available are $M_e = M - m$, increasing the average spectral efficiency r_e . Apart from that, the analysis presented in remainder of the paper is still valid in this case. We also remark that the maximum number of recoverable punctured mini-slots m is $M - 1$, to leave at least one mini-slot to the eMBB data transmission. On the other hand, for the general OMA and NOMA schemes presented so far, the URLLC data stream can be transmitted to all M mini-slots. Therefore, a performance comparison between puncturing, OMA, and NOMA is unfair, and we focus on comparing OMA and NOMA only.

2.1 Signal model

We consider a multi-carrier system, where a single mRB (t, f) , corresponds to mini-slot $t \in \mathcal{M}$ and frequency resource $f \in \mathcal{F}$. Depending on the multiple access technology, each resource can be used simultaneously by both e and u users (NOMA) or by only one of them (OMA). In any case, the corresponding signals, denoted as $\mathbf{s}_e(t, f)$ for user e and as $\mathbf{s}_u(t, f)$ for user u , satisfies the following requirements

$$\mathbb{E} \{ \|\mathbf{s}_e(t, f)\|^2 \} = 1, \quad \mathbb{E} \{ \|\mathbf{s}_u(t, f)\|^2 \} = 1, \quad \mathbb{E} \{ \mathbf{s}_e^H(t, f) \mathbf{s}_u(t, f) \} = 0.$$

We remark that URLLC codewords are exactly contained in a single transmission, spanning contiguous mini-slots. In this way, if M_u is chosen appropriately, a single successful transmission carries all the information to the receiver, fulfilling the latency constraint. On the other hand, the eMBB codewords may span the whole time-slot since they do not have any specific latency constraints. In the case of NOMA, the decoding process implies that one of the two users employs SIC to remove the data stream of the other (interfering) user. However, the cancellation of a user's data stream requires the reception of the entire codeword. Since eMBB codewords span an indeterminate number of mini-slots, the URLLC user that waits for the reception of the whole e codeword may incur a violation of its latency requirements. Therefore, we adopt a NOMA paradigm where it is always the eMBB user that employs the SIC to remove the interference, and the URLLC will always be received in the presence of the eMBB interference.

The base station (BS) transmits both eMBB and URLLC data streams using superposition coding. The transmitted signal in an mRB (t, f) is:

$$\mathbf{x}(t, f) = \sqrt{P_e(t, f)} \mathbf{s}_e(t, f) + \sqrt{P_u(t, f)} \mathbf{s}_u(t, f) \quad (3)$$

where $P_e(t, f)$, $P_u(t, f)$ are the power coefficient used to transmit the symbols of e and u on resource (t, f) , respectively. It is worth noting that this formalization implies the possibility of the transmission of the data stream of a single user $i \in \{u, e\}$ in an OMA fashion by setting the power coefficient of one of the two users equal to 0. We further denote as \mathbf{P}_e and \mathbf{P}_u the vectors collecting all the eMBB and URLLC power coefficients, respectively.

On the receiver side, we can model the signal received by user $i \in \{e, u\}$ as

$$\mathbf{y}_i(t, f) = h_i(f) \mathbf{x}(t, f) + \mathbf{n}_i \quad (4)$$

where $h_i(f)$, $i \in \{e, u\}$, is the fading channel gain taking into account both small-scale and large-scale fading, and $n_i \sim \mathcal{N}(0, \sigma^2 \mathbf{I}_n)$, $i \in \{e, u\}$, is the noise at the receiver. Specifically, $h_e(f)$ realization is assumed known at the transmitter, while $h_u(f)$ is assumed unknown. We remark that the channel fading coefficient will not change during the whole slot, leading to the dependence of frequency only. In the remainder of the paper, we assume a Rayleigh fading; however, this assumption is not essential, and all the consideration can be extended for other kinds of fading. To simplify the notation, we further denote the normalized instantaneous SNR at the receiver $i \in \{e, u\}$ as

$$\gamma_i(f) = \frac{|h_i(f)|^2}{\sigma^2} \quad (5)$$

where $\gamma_i(f) \sim \text{Exp}(\Gamma_i)$ in case of Rayleigh fading, with $\gamma_e(f)$ known, while $\gamma_u(f)$ unknown. In the remainder of the paper, we denote as $\Gamma_i = \mathbb{E}\{\gamma_i\}$, $i \in \{e, u\}$ the normalized mean SNR at the receiver.

2.2 Mutual information

Due to the transmission of short packets for the URLLC communication, the model of the communication is accurately addressed by the finite blocklength regime [18]. For this regime, the back-off from the channel capacity is characterized by the so-called channel dispersion, which measures the stochastic variability of the channel. Fortunately, in the case of quasi-static channels, the channel dispersion is zero, regardless if the CSI is known or not at the transmitter [19]. Hence, the performance of our system may be evaluated by means of outage capacity, even if the blocklength of transmitted data does not go to infinity [20].

To reliably transmit the data stream requested by the users, we have to guarantee that the accumulated mutual information of each transmission is high enough to sustain the target rate r_i , $i \in \{e, u\}$, with high probability. According to the previous definitions, the mutual information of u data stream at receiver u is [21]

$$I_u(\mathbf{P}_u, \mathbf{P}_e) = \frac{1}{F_u M_u} \sum_{t \in \mathcal{M}_u} \sum_{f \in \mathcal{F}_u} \log_2 \left(1 + \frac{\gamma_u(f) P_u(t, f)}{1 + \gamma_u(f) P_e(t, f)} \right); \quad [\text{bit/s/Hz}] \quad (6)$$

the mutual information of u data stream at receiver e is

$$I_{u,e}(\mathbf{P}_u, \mathbf{P}_e) = \frac{1}{F_u M_u} \sum_{t \in \mathcal{M}_u} \sum_{f \in \mathcal{F}_u} \log_2 \left(1 + \frac{\gamma_e(f) P_u(t, f)}{1 + \gamma_e(f) P_e(t, f)} \right), \quad [\text{bit/s/Hz}] \quad (7)$$

needed to address the SIC process. Note that $I_{u,e} = 0$ in the OMA case, accordingly. Finally, the mutual information of e data stream at receiver e after a successful SIC process is

$$I_e(\mathbf{P}_e) = \frac{1}{F_e M_e} \sum_{t \in \mathcal{M}_e} \sum_{f \in \mathcal{F}_e} \log_2 (1 + \gamma_e(f) P_e(t, f)). \quad [\text{bit/s/Hz}] \quad (8)$$

where SIC process is always assumed successful in the OMA case, to consider a coherent model for both multiple access paradigms.

We remark that the same instantaneous SNR $\gamma_i(f)$ for the different mini-slots leads to a linear dependence between the mutual information and the number of mini-slots spanned by the transmission. If the mutual information transmitting onto F_i frequencies and M_i mini-slots is denoted as I , expanding that transmission onto kM_i mini-slots with the same power coefficients will result in a mutual information of kI , $\forall k \in \mathbb{N}^{++}$. On the other hand, the diversity gain obtained by spanning more frequencies is not easily addressable. To the best of our knowledge, the only concise expression for the diversity gain for parallel channels is given in [14], which depends on the fading distribution. However, the approximation defined in [14] is valid only if the same power (signal and inference) is used on all channels; therefore, it cannot be applied in this framework.

2.3 Outage events

Given the mutual information denoted above, it is easy to define the outage events that may occur during the transmission towards both users.

Let us start from the outage events occurring at e . The data stream transmitted to e is incorrectly decoded if: the SIC process is not successful, or the data stream of e is erroneously decoded after the SIC. The SIC process cannot be successfully employed if $r_u > I_{u,e}$, and its probability is

$$p_{u,e}(\mathbf{P}_u, \mathbf{P}_e) = \Pr\{I_{u,e}(\mathbf{P}_u, \mathbf{P}_e) < \eta_u\}. \quad (9)$$

Assuming that the SIC process has been successful, the data stream of e is wrongly decoded at its own receiver if $r_e > I_e$, which occurs with probability

$$p_e(\mathbf{P}_e) = \Pr\{I_e(\mathbf{P}_e) < r_e\}. \quad (10)$$

It is worth noting that the assumption of complete knowledge of the CSI for the eMBB user constraints p_e and $p_{u,e}$ to be either 1 or 0.

Let us now focus on the outage event for u . The data stream intended for u is not successfully decoded if the URLLC packet is erroneously decoded at receiver u , happening if $r_u > I_u$, or the URLLC packet is not entirely received before the latency requirement M_u^{\max} . Defining the waiting time W_u as the number of mini-slots not used by u between the arrival and the complete transmission of the URLLC packet, the outage probability of u can be formalized as [20]

$$p_u(\mathbf{P}_u, \mathbf{P}_e) = \Pr\{I_u(\mathbf{P}_u, \mathbf{P}_e) \leq r_u \cup W_u + M_u > M_u^{\max}\}. \quad (11)$$

Using Boole's inequality, the outage probability can be upper bound by

$$p_u(\mathbf{P}_u, \mathbf{P}_e) \leq \Pr\{I_u(\mathbf{P}_u, \mathbf{P}_e) \leq r_u\} + \Pr\{M_u > M_u^{\max} - W_u\} \leq \epsilon_u, \quad (12)$$

which must be lower than the URLLC reliability constraint ϵ_u . The latency term in (12) can be constrained to be 0 choosing a reasonable value of M_u , such as

$$M_u \leq M_u^{\max} - W_u. \quad (13)$$

Since channel gains are static on the time dimension, the set \mathcal{M}_u can be chosen randomly between all the possible sets guaranteeing relation (13). According to the definition of spectral efficiency (2), spreading the same number of informative bits on more than one mini-slot directly reduces the target rate r_u . Hence, a way to reduce the transmission power is exploiting the tolerable delay as much as possible. Nevertheless, it is worth noting that using a large value of M_u for the transmission of a packet may prevent the transmission of the following URLLC packet, increasing the latency experienced by the latter. Thus, we want to stress the fact that a complete design of the transmission time should also take into account the URLLC traffic model and parameter, which is beyond the scope of this investigation. In the remainder, we address the problem of minimum power assuming M_u is given. Therefore, we allocate the power coefficients to guarantee that the mutual information I_u can sustain the rate r_u with probability $1 - \epsilon_u$.

3 Resource allocation

Following the previous definition, we can formalize the overall minimum power allocation problems for both OMA and NOMA scheme. We further define as $P^{\text{tot}} = \sum_{t \in \mathcal{M}} \sum_{f \in \mathcal{F}} P_u(t, f) + P_e(t, f)$ the overall power spent.

For the OMA power allocation problem, we combine together the eMBB decoding requirement (10), the reliability requirement (11), and the orthogonality of resource allocation. Hence, the OMA problem is the following

$$\min_{\mathbf{P}_e, \mathbf{P}_u} P^{\text{tot}} \quad (14)$$

$$\text{s.t. } p_e(\mathbf{P}_e) = 0, \quad (14.a)$$

$$P_u(t, f)P_e(t, f) = 0, \forall t \in \mathcal{M}, \forall f \in \mathcal{F} \quad (14.b)$$

$$p_u(\mathbf{P}_u, \mathbf{P}_e) \leq \epsilon_u, \quad (14.c)$$

$$\mathbf{P}_u \succeq 0, \mathbf{P}_e \succeq 0, \quad (14.d)$$

where constraint (14.b) denotes the orthogonality of the allocation process. On the other hand, the NOMA allocation problem is almost identical, where the orthogonality constraint is substituted by the SIC requirement. Hence, the minimization problem results

$$\min_{\mathbf{P}_e, \mathbf{P}_u} P^{\text{tot}} \quad (15)$$

$$\text{s.t. } p_e(\mathbf{P}_e) = 0, \quad (15.a)$$

$$p_{u,e}(\mathbf{P}_u, \mathbf{P}_e) = 0, \quad (15.b)$$

$$p_u(\mathbf{P}_u, \mathbf{P}_e) \leq \epsilon_u, \quad (15.c)$$

$$\mathbf{P}_u \succeq 0, \mathbf{P}_e \succeq 0. \quad (15.d)$$

Problems (14) and (15) are not convex w.r.t. both \mathbf{P}_u and \mathbf{P}_e . Moreover, the evaluation of (14.c) and (15.c) are not known, and only bound or approximations can be used, e.g. see [13, 14, 16]. Unfortunately, these approximations are not convex and special function are involved. Thus, optimize both the power coefficients using these approximations is an hard task.

In the following, we show that a solution to the problem can be obtained by decoupling the overall problem for \mathbf{P}_e and \mathbf{P}_u to solve simpler convex problems. In particular, we minimize the eMBB power subject to its decoding process (10); then, we found the minimum URLLC power guaranteeing SIC process (9); finally, we evaluate the URLLC power allocation constrained to (11). In the following Subsections, the decoupled problems are presented. Then, in Section 4, we will describe the overall procedure for the power allocation.

3.1 eMBB allocation

Let us start with the eMBB allocation. In the time domain, the allocation is defined by the 5G NR standard, specifying that the eMBB transmission should be allocated to an entire slot, i.e., $\mathcal{M}_e = \mathcal{M}$, $M_e = M$. On the spectral domain, we assume that the number of frequencies spanned by the URLLC transmission F_u has been selected in some way¹, resulting in knowing exactly the number of resources F_u and F_e reserved to both users. Therefore, it is easy to find the set of frequencies to be used by the eMBB data transmission. The mutual information I_e defined in (8) depends only on the power coefficients \mathbf{P}_e for both OMA and NOMA case; it is maximized if the set \mathcal{F}_e contains the frequencies with highest instantaneous SNR $\gamma_e(f)$ among the possible ones, or equivalently the set F_u will contain the mRB with lowest channel gains. Hence, the set of frequency resources given to u is

$$\mathcal{F}_u = \arg \min_{\mathcal{F}'_u \subseteq \mathcal{F}, |\mathcal{F}'_u| = F_u} \sum_{f \in \mathcal{F}'_u} \gamma_e(f), \quad (16)$$

and the set of resources for e can be computed following (1). We remark that this mRB selection does not influence the URLLC transmission, not knowing the CSI for those channels.

The power coefficient chosen for a particular mRB will be the same in every mini-slot, because of the quasi-static channel gains and no interference experienced (see eq. (8)). More formally, $P_e(t, f) = P_e(f)$, $\forall t \in \mathcal{M}$, $\forall f \in \mathcal{F}$, and eq. (8) can be simplified in:

$$I_e(\mathbf{P}_e) = \frac{1}{F_e} \sum_{f \in \mathcal{F}_e} \log_2(1 + \gamma_e(f)P_e(f)). \quad (17)$$

Following the above assumptions, we can obtain the minimum power spent guaranteeing $p_e = 0$, solving the following problem

$$\begin{aligned} \min_{\mathbf{P}_e \succeq 0} \quad & \sum_{f \in \mathcal{F}_e} P_e(f) \\ \text{s.t.} \quad & \sum_{f \in \mathcal{F}_e} \log_2(1 + \gamma_e(f)P_e(f)) \geq F_e r_e. \end{aligned} \quad (18)$$

The solution of problem (18) can be computed through the well-known water-filling approach [21], obtaining the desired power coefficients \mathbf{P}_e as

$$P_e(f) = \begin{cases} 2^{r_e \frac{F_e}{F_e^+}} \prod_{i \in \mathcal{F}_e^+} \left(\frac{1}{\gamma_e(i)} \right)^{\frac{1}{F_e^+}} - \frac{1}{\gamma_e(f)}, & f \in \mathcal{F}_e^+ \\ 0, & \text{otherwise} \end{cases} \quad (19)$$

where the set $\mathcal{F}_e^+ \subseteq \mathcal{F}_e$, $|\mathcal{F}_e^+| = F_e^+$, is composed by all and only the mRBs that guarantees $P_e(f) > 0$, $\forall f \in \mathcal{F}_e^+$ [22].

In a similar way, following the definition (7), we can obtain the minimum power spent to transmit the URLLC packet satisfying the SIC requirement, i.e. $p_{u,e} = 0$. The problem become

$$\begin{aligned} \min_{\mathbf{P}_u \succeq 0} \quad & \sum_{f \in \mathcal{F}_u} P_u(f) \\ \text{s.t.} \quad & \sum_{f \in \mathcal{F}_u} \log_2 \left(1 + \frac{\gamma_e(f)P_u(f)}{1 + \gamma_e(f)P_e(f)} \right) \geq F_u r_u. \end{aligned} \quad (20)$$

¹In Section 5 different choices of the number of frequencies are compared.

Also in this case, a water-filling approach may be employed considering the channels involved in the optimization are $\frac{\gamma_e(f)}{1+\gamma_e(f)P_e(f)}$. The solution obtained is labeled as $\mathbf{P}_u^{\text{SIC}}$ to highlight the fact that this is the minimum power needed to satisfy the SIC constraint, whose components are

$$P_u^{\text{SIC}}(f) = \begin{cases} 2^{r_u \frac{F_u}{F_u^+}} \prod_{i \in \mathcal{F}_u^+} \left(\frac{1}{\gamma_e(i)} + P_e(i) \right)^{\frac{1}{F_u^+}} - \frac{1}{\gamma_e(f)} - P_e(f), & f \in \mathcal{F}_u^+, \\ 0, & \text{otherwise} \end{cases} \quad (21)$$

where $\mathcal{F}_u^+ \subseteq \mathcal{F}_u$, $|\mathcal{F}_u^+| = F_u^+$, collects all and only the mRBs reserved for u guaranteeing $P_u^{\text{SIC}}(f) > 0$. To address the lack of SIC process for the OMA paradigm, we impose $\mathcal{F}_u^+ = \emptyset$, resulting in $\mathbf{P}_u^{\text{SIC}} = \mathbf{0}$.

It is worth noting that the power coefficient obtained in (21) will be used as the minimum value for the evaluation of the optimal power coefficient for the transmission of u data stream to receiver u . In this way, we guarantee the SIC requirement on the eMBB user. We remark that $P_u^{\text{SIC}}(f)$ depends on the set \mathcal{F}_u^+ : the higher is the cardinality F_u , the higher will be F_u^+ , and the lower is the power spent. Moreover, better eMBB channel gain conditions lead to a lower power consumption for SIC process due to higher $\gamma_e(f)$ and lower $P_e(f)$ given by (19). On the other hand, when the eMBB user experiences poor channel condition, the SIC process may be the dominant effect in the allocation of URLLC power, as we show in Section 5.

3.2 URLLC allocation

We now focus on the power allocation of the URLLC user guaranteeing its quality of service. Following relation (13), we know in advance the set of mini-slot \mathcal{M}_u in which the URLLC packet is transmitted, and we only need to focus on the reliability problem. Therefore eq. (11) can be rewritten as

$$p_u(\mathbf{P}_u) = \Pr \{I_u(\mathbf{P}_u) \leq r_u\} \leq \epsilon_u, \quad (22)$$

where we highlighted the dependence on \mathbf{P}_u only, assuming that the power coefficients for the eMBB user are already been evaluated by solution (19). Also for this case, we can obtain all the power coefficients studying a single mini-slot. The eMBB interference power coefficients depend on the frequency only, being the same for different mini-slots. Having same interference and channel gain - even if unknown -, the power coefficient for URLLC transmission will depends on frequency only, i.e. $P_u(t, f) = P_u(f)$, $t \in \mathcal{M}_u$, $f \in \mathcal{F}_u$. Thus, the mutual information I_u can be simplified in:

$$I_u(\mathbf{P}_u) = \frac{1}{F_u} \sum_{f \in \mathcal{F}_u} \log_2 \left(1 + \frac{\gamma_u(f)P_u(f)}{1 + \gamma_u(f)P_e(f)} \right). \quad (23)$$

Taking into account both constraints on the SIC process and reliability requirement, we can now express the URLLC allocation problem as follows

$$\begin{aligned} & \min_{\mathbf{P}_u \succeq \mathbf{P}_u^{\text{SIC}}} \sum_{f \in \mathcal{F}_u} P_u(f), \\ & \text{s.t. } \Pr \left\{ \sum_{f \in \mathcal{F}_u} \log_2 \left(1 + \frac{\gamma_u(f)P_u(f)}{1 + \gamma_u(f)P_e(f)} \right) \leq F_u r_u \right\} \leq \epsilon_u. \end{aligned} \quad (24)$$

In theory, the minimization of the objective function of (24) may be obtained by applying a gradient descent approach, if the chosen power coefficients always lie in the feasible set. Nevertheless, due to the unknown formulation of the outage probability, projection [23] or conditional gradient descent algorithms [24] cannot be applied directly.

In the following, we show an analytic solution of problem (24) for two particular cases - single frequency and interference-limited scenario.

3.2.1 Single frequency resource

When a single frequency resource is allocated, i.e. $F_u = 1$, the resolution of (22) is known [15], and the minimum transmission power can be obtained imposing $p_u = \epsilon_u$. For a Rayleigh fading, we obtain

$$P_u^{\text{single}}(f) = \begin{cases} (2^{r_u} - 1) \left(P_e(f) - \frac{1}{\Gamma_u \ln(1 - \epsilon_u)} \right), & f \in \mathcal{F}_u, \\ 0, & \text{otherwise.} \end{cases} \quad (25)$$

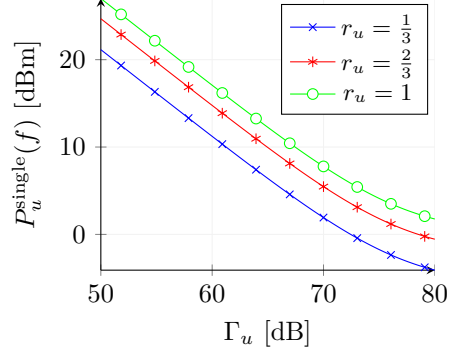


Figure 2: $P_u^{\text{single}}(f)$ as a function of Γ_u according to (25), when $\epsilon_u = 10^{-5}$ and $P_e(f) = 0$ dBm.

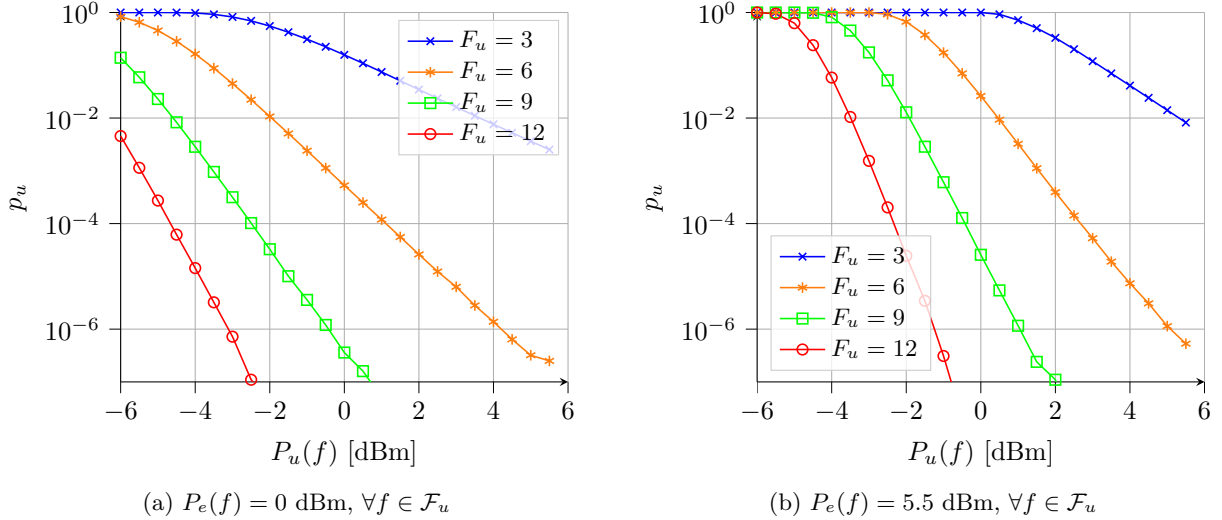


Figure 3: Experimental results of p_u (22) versus $P_u(f)$ with different number of F_u , $F_u r_u = 1$, $\Gamma_u = 30$ dB and $P_u(f) = P_u$, $\forall f \in \mathcal{F}_u$.

In Fig. 2, we show $P_u^{\text{single}}(f)$ as a function of the mean normalized SNR Γ_u . The reliability is set as $\epsilon_u = 10^{-5}$ and $P_e(f) = 0$ dBm. If $r_u = 1/3$, we need $\Gamma_u \geq 61$ dB to have $P_u^{\text{single}}(f) \leq 10$ dBm meeting the requirements. Hence, the use of a single frequency resource can be only used when the user experiences very good channel conditions, due to close distance from the BS or favorable scattering scenario. When $F_u > 1$, the exact evaluation of the probability presented in (22) is not known. Experimental results prove that increasing the available frequency resources will lead to a great improvement in terms of reliability, as shown in Fig. 3. In other words, in a general case when the channel conditions are not good enough, we must rely on the diversity gain provided by using multiple frequencies.

3.2.2 Interference-limited scenario

A bound of the power consumption for URLLC in the NOMA case can be found exploiting the asymptotic behavior with respect to $\gamma_u(f)$. When the URLLC channel conditions are very good, we can approximate each term of (23) depending on the value of the interference. In details, let us consider the mRB $f \in \mathcal{F}_u$ where the interference is not null, i.e. $P_e(f) > 0$. The mutual information of that channel can be approximated as

$$\log_2 \left(1 + \frac{\gamma_u(f)P_u(f)}{1 + \gamma_u(f)P_u(f)} \right) \xrightarrow{\Gamma_u \rightarrow \infty} \log_2 \left(1 + \frac{P_u(f)}{P_e(f)} \right). \quad (26)$$

On the other hand, considering a mRB $g \in \mathcal{F}_u$ where the interference is null, i.e. $P_e(g) = 0$, the contribution of its term in the summation can be approximated by

$$\log_2 (1 + \gamma_u(f)P_u(f)) \xrightarrow{\Gamma_u \rightarrow \infty} \log_2 (\gamma_u(f)P_u(f)). \quad (27)$$

Using the set definition given in Section 3.1, the mRBs having $P_e(f) > 0$ are collected in the set $\mathcal{F}_u \cap \mathcal{F}_e^+$, i.e. the URLLC reserved frequencies shared with \mathcal{F}_e^+ ; the mRBs having $P_e(f) = 0$ are collected in the set $\mathcal{F}_u \setminus \mathcal{F}_e^+$, i.e. the URLLC reserved frequency resources which are not in the set \mathcal{F}_e^+ . Therefore, equation (23) can be well approximated by the following

$$F_u I_u(\mathbf{P}_u) \approx \sum_{f \in \mathcal{F}_u \cap \mathcal{F}_e^+} \log_2 \left(1 + \frac{P_u(f)}{P_e(f)} \right) + \sum_{f \in \mathcal{F}_u \setminus \mathcal{F}_e^+} \log_2 (\gamma_u(f) P_u(f)). \quad (28)$$

The summation of terms involving no interference leads to a formulation of the outage probability, which can be tightly bounded using the approach given in [13]. However, this bound is still very complicated and make use of special function, while we are interested in a simple formulation suggesting the behavior of the power allocation for the interference-limited case. To overcome this, we note that the term (27) has a high probability of being greater than the biggest term of (26). In other words, if we consider the mRB with the lowest interference greater than 0, i.e.,

$$f^{\min} = \arg \min_{f \in \mathcal{F}_u \cap \mathcal{F}_e^+} P_e(f), \quad (29)$$

the probability that each realization of the SNR in $\mathcal{F}_u \setminus \mathcal{F}_e^+$ is greater than the lowest interference is

$$\prod_{f \in \mathcal{F}_u \setminus \mathcal{F}_e^+} \Pr \left\{ \gamma_u(f) \geq \frac{1}{P_e(f^{\min})} \right\} = e^{-\frac{|\mathcal{F}_u \setminus \mathcal{F}_e^+|}{\Gamma_u P_e(f^{\min})}} \xrightarrow{\Gamma_u \rightarrow \infty} 1, \quad (30)$$

for i.i.d. Rayleigh fading. Therefore, we can substitute $1/P_e(f^{\min})$ to all the channels experiencing no interference $\mathcal{F}_u \setminus \mathcal{F}_e^+$. In this way, we obtain an approximate formulation which is a lower bound of (28) almost surely.

To summarized, when the system is interference-limited, equation (23) is bounded with high probability by

$$I_u(\mathbf{P}_u) \geq \tilde{I}_u(\mathbf{P}_u) = \frac{1}{F_u} \sum_{f \in \mathcal{F}_u} \log_2 \left(1 + \frac{P_u(f)}{P_e(f)} \right), \quad (31)$$

where it is implied that $P_e(f) = P_e(f^{\min})$, $\forall f \in \mathcal{F}_u \setminus \mathcal{F}_e^+$. Hence, finding the power coefficients \mathbf{P}_u guaranteeing $\tilde{I}_u(\mathbf{P}_u) \geq r_u$, we obtain that $\Pr\{I_u(\mathbf{P}_u) \geq r_u\} \rightarrow 1$.

Using (31), the minimum power coefficients can be found solving the following problem

$$\begin{aligned} \min_{\mathbf{P}_u \succeq 0} \quad & \sum_{f \in \mathcal{F}_u} P_u(f) \\ \text{s.t.} \quad & \sum_{f \in \mathcal{F}_u} \log_2 \left(1 + \frac{P_u(f)}{P_e(f)} \right) \geq F_u r_u. \end{aligned} \quad (32)$$

Using the water-filling approach, setting the channel gain of each mRB as $1/P_e(f)$, we obtain

$$P_u^{\text{IL}}(f) = \begin{cases} 2^{r_u F_u} \prod_{i \in \mathcal{F}_u} P_e(i)^{\frac{1}{F_u}} - P_e(f), & f \in \mathcal{F}_u, \\ 0, & \text{otherwise.} \end{cases} \quad (33)$$

Solution (33) leads to a vector \mathbf{P}_u^{IL} which guarantees that $\tilde{I}_u(\mathbf{P}_u^{\text{IL}}) \geq r_u$ for the interference-limited scenario. In the numerical results, we show that the interference-limited scenario may occur when the eMBB user is the farther user. In this kind of scenarios, \mathbf{P}_u^{IL} (33) can be used efficiently for the URLLC allocation.

4 Simplified solutions for power allocation

As already said, a closed form of eq. (22) cannot be evaluated. However, we may state a non-increasing property of the outage probability which is useful for the proposed simplified solutions.

Proposition 1. *Assuming fixed values of r_u , and \mathbf{P}_e , the outage probability (22) is a non-increasing monotone function.*

Proof. The log function is monotonic non-decreasing w.r.t. each $P_u(f)$. Hence, reducing the power coefficient on a single mRB keeping the other power terms unchanged will reduce the mutual information I_u . More formally, if we consider the vector \mathbf{P}'_u obtained decreasing $P_u(f)$, $f \in \mathcal{F}_u$, by $\delta > 0$, while the other $P_u(g)$, $\forall g \in \mathcal{F}_u \setminus \{f\}$, and $P_e(j)$, $\forall j \in \mathcal{F}_u$, are kept the same, the mutual information results

$$F_u I_u(\mathbf{P}'_u) = \log_2 \left(1 + \frac{\gamma_u(f)(P_u(f) - \delta)}{1 + \gamma_u(f)P_e(f)} \right) + \sum_{g \in \mathcal{F}_u \setminus \{f\}} \log_2 \left(1 + \frac{\gamma_u(g)P_u(g)}{1 + \gamma_u(g)P_e(g)} \right) \leq F_u I_u(\mathbf{P}_u). \quad (34)$$

Therefore, the outage probability may only result larger (or equal), i.e.,

$$p_u(\mathbf{P}'_u) = \Pr\{I_u(\mathbf{P}'_u) \leq r_u\} \geq p_u(\mathbf{P}_u) = \Pr\{I_u(\mathbf{P}_u) \leq r_u\}. \quad (35)$$

The same relation is in fact extended for each $\mathbf{P}'_u \succeq 0$ such as $\mathbf{P}'_u \preceq \mathbf{P}_u$, which completes the proof. \square

Moreover, we will make use of a look-up table based on Monte Carlo simulations for the estimation of the outage probability. From eq. (22), we can see that the outage probability depends on r_u , Γ_u , \mathcal{F}_u , \mathbf{P}_e and \mathbf{P}_u . In theory, we can tabulate the outage probability varying these parameters. However, populating the table for all the possible vectors \mathbf{P}_e and \mathbf{P}_u will lead to a huge number of trials and a huge dimension of the table itself. Furthermore, the complexity increases with the number of frequencies employed, obtaining bigger tables for greater frequency sets. To overcome these problems, we tabulate the outage probability assuming that the same P_u and the same P_e are used for all the considered mRBs. Let us denote as

$$\hat{p}_u(P_u, P_e, \Gamma_u, \mathcal{F}_u, r_u) = \lim_{n \rightarrow \infty} \frac{1}{n} \sum_{i=1}^n \mathbb{1} \left\{ \sum_{f \in \mathcal{F}_u} \log \left(1 + \frac{P_u \gamma_u(f)}{1 + P_e \gamma_u(f)} \right) \leq F_u r_u \right\} \quad (36)$$

the Monte Carlo estimation of the outage probability p_u when $P_u(f) = P_u$ and $P_e(f) = P_e \forall f \in \mathcal{F}_u$, where $\mathbb{1}\{\cdot\}$ is the indicator function. From now on, we will recall eq. (36) to address the whole look-up table, for simplicity.

In the remainder of the section, we exploit the previous findings to propose two different algorithms able to solve both the OMA and NOMA allocation problems (14)-(15).

4.1 Feasible solution for URLLC power

A feasible solution for the power minimization constrained to the multi-carrier outage probability can be obtained employing the look-up table (36). Given the known values Γ_u , r_u and F_u , we load the portion of the table concerning these parameters $\hat{p}_u(\cdot, \cdot, \Gamma_u, \mathcal{F}_u, r_u)$. Then, we compute the eMBB power coefficients $P_e(f)$ through (19). In order to found the feasible power P_u , we consider the mRB experiencing the worst interference, denoted as

$$f^{\max} = \arg \max_f P_e(f). \quad (37)$$

Then, from tabulated $\hat{p}_u(\cdot, \cdot, \Gamma_u, \mathcal{F}_u, r_u)$, we extract the minimum P_u that guarantees the outage probability when the interference is given by $P_e(f^{\max})$, i.e.

$$P_u = \min \{P \mid \hat{p}_u(P, P_e(f^{\max}), \Gamma_u, \mathcal{F}_u, r_u) \leq \epsilon_u\}. \quad (38)$$

In other words, we found the feasible power needed for the transmission assuming that all channels experience the strongest interference. Finally, we set:

$$P_u^*(f) = \max \{P_u, P_u^{\text{SIC}}(f)\}, \quad \forall f \in \mathcal{F}_u. \quad (39)$$

The procedure is summarized in Algorithm 1. In the following, we show that this algorithm provides a feasible solution for the allocation process.

Proposition 2. *Algorithm 1 guarantees a feasible solution of OMA allocation problem (14) and NOMA allocation problem (15).*

Proof. In the case of OMA, from the definition of \mathcal{F}_e (1), we have $\mathcal{F}_u \cap \mathcal{F}_e = \emptyset$, and the orthogonality requirement is satisfied by definition. In any case, computing the eMBB power coefficient through eq. (19) guarantees that $p_e = 0$ [25]. Moreover, power coefficient P_u is the minimum power ensuring $\hat{p}_u(P_u, P_e(f^{\max}), \Gamma_u, \mathcal{F}_u, r_u) \leq \epsilon_u$. In other words, a transmission onto F_u mRBs, employing power coefficients P_u , and interference coefficients $P_e(f^{\max})$, has outage probability $p_u \leq \epsilon_u$. Taking into account

that $P_e(f^{\max}) \geq P_e(f)$, $\forall f \in \mathcal{F}_u$, we obtain that the mutual information (6) evaluated with URLLC power coefficient P_u for all mRBs and the actual interference coefficient \mathbf{P}_e is greater (or equal) than the mutual information having interference $P_e(f^{\max})$, i.e.

$$I_u(P_u, \mathbf{P}_e) \geq I_u(P_u, P_e(f^{\max})).$$

Furthermore, operator (39) assures that the power coefficient is increased to meet the minimum power needed for the SIC if needed. Again, this operation can only increase the mutual information, obtaining

$$I_u(\mathbf{P}_u^*, \mathbf{P}_e) \geq I_u(P_u, \mathbf{P}_e) \geq I_u(P_u, P_e(f^{\max})). \quad (40)$$

At the same time, operator (39) assures the SIC requirement, i.e. $p_{u,e} = 0$. We remark that eq. (40) is deterministically valid because the channel realizations are the same in both left and right side hands of the relation. Using (22) we can evaluate the probability of being in outage, which will follow

$$p_u = \Pr \{I_u(\mathbf{P}_u^*, \mathbf{P}_e) \leq r_u\} \leq \Pr \{I_u(P_u, P_e(f^{\max})) \leq r_u\} \leq \epsilon_u, \quad (41)$$

satisfying the reliability constraint. \square

It is worth noting that this scheme is generally sub-optimal in terms of power spent, considering that we constraint all channels to act as the worst one. On the other hand, for OMA allocation, we can demonstrate the following proposition.

Proposition 3. *Given Γ_u , \mathcal{F}_u , and r_u , if the look-up table (36) contains an entry where $\hat{p}_u(P_u, 0, \Gamma_u, \mathcal{F}_u, r_u) = \epsilon_u$ exactly, Algorithm 1 provide the optimal solution of the URLLC OMA allocation problem (24), and the optimal power coefficient is $P_u^*(f) = P_u$, $\forall f \in \mathcal{F}_u$.*

Proof. For the OMA allocation, the power coefficient of e user is zero for every resources given to u , i.e. $P_e(f) = 0$, $\forall f \in \mathcal{F}_u$. In these conditions of i.i.d. parallel channels without interference, the minimum outage probability is reached when the same power coefficient is allocated to each channel [21]. As a matter of fact, Algorithm 1 outputs the power coefficient P_u given by (38) for each mRB, due to the lack of SIC constraint for the OMA case. The resulting vector $\mathbf{P}_u^* = [P_u, \dots, P_u]^T$ is at least a feasible solution of problem (14), due to Proposition 2. The resulting mutual information is

$$I_u(\mathbf{P}_u^*, \mathbf{P}_e) = I_u(P_u, 0) = \frac{1}{F_u} \sum_{f \in \mathcal{F}_u} \log_2(1 + \gamma_u(f)P_u).$$

Proposition 1 is a generalization of this particular case; thus, the outage probability $p_u(\mathbf{P}_u^*)$ is monotonically non-increasing in P_u . Having obtained P_u following (38), there is no other power coefficient $P'_u \leq P_u$ such as $\hat{p}_u(P'_u, 0, \Gamma_u, \mathcal{F}_u, r_u) \leq \epsilon_u$. Eventually, if the table has been populated with enough different values of P_u , we will find that $p_u(P_u, 0, \Gamma_u, \mathcal{F}_u, r_u) = \epsilon_u$, and the optimal solution is reached. \square

In a practical approach, Proposition 3 means that the solution given by Algorithm 1 is reasonably close to the optimal one for the OMA allocation. More P_u values are tested in the look-up table (36) closer to the optimal results we get.

Algorithm 1: Feasible algorithm (N-fea)

- 1 **Initialize:** Having populated the table $\hat{p}_u(P_u, P_e, \Gamma_u, \mathcal{F}_u, r_u)$;
 - 2 Compute \mathbf{P}_e through (19);
 - 3 Compute $\mathbf{P}_u^{\text{SIC}}$ through (21);
 - 4 $f^{\max} = \arg \max_f P_e(f)$;
 - 5 $P_u = \min\{P_u \mid \hat{p}_u(P_u, P_e(f^{\max}), \Gamma_u, \mathcal{F}_u, r_u) \leq \epsilon_u\}$;
 - 6 **for** $f \in \mathcal{F}_u$ **do**
 - 7 $P_u^*(f) = \max\{P_u, P_u^{\text{SIC}}(f)\}$;
 - 8 **Output:** \mathbf{P}_u^*
-

4.2 Constrained block coordinated descent optimization

To overcome the sub-optimality given by Algorithm 1, we propose an iterative algorithm based on BCD optimization, a class of algorithms able to effectively solve large-scale optimization problems [26, 27]. The main idea is based on non-increasing property of the outage probability (22) given in Proposition 1.

For each iteration, we update the power coefficients one after another, following a deterministic order. Without loss of generality, we assume that the predetermined order is the natural order of set \mathcal{F}_u , i.e., $0, 1, 2, \dots, F_u - 1$. To take into account the dimension-wise updating process, we denote the power coefficient vector at iteration i where the first $f \in \mathcal{F}_u$ terms have been updated as

$$\mathbf{P}_u^{(i,f)} = [P_u^{(i)}(0), \dots, P_u^{(i)}(f-1), P_u^{(i-1)}(f), \dots, P_u^{(i-1)}(F_u-1)]^T. \quad (42)$$

The aim is updating each power coefficient only if the resulting outage probability satisfy the reliability requirement. To guarantee the feasibility of using $\mathbf{P}_u^{(i,f)}$, the power coefficient of frequency component $f \in \mathcal{F}_u$ is updated as follows

$$P_u^{(i)}(f) = \begin{cases} \max \left\{ P_u^{\text{SIC}}(f), P_u^{(i-1)}(f) - \mu^{(i)} \right\}, & \text{if } \hat{p}_u(\mathbf{P}_u^{(i,f)}, \mathbf{P}_e, \Gamma_u, \mathcal{F}_u, r_u) \leq \epsilon_u, \\ P_u^{(i-1)}(f), & \text{otherwise,} \end{cases} \quad (43)$$

where $\mu^{(i)} > 0$ is the step size at iteration i , $\hat{p}_u(\mathbf{P}_u^{(i,f)}, \mathbf{P}_e, \Gamma_u, \mathcal{F}_u, r_u)$ is the Monte Carlo estimation of the outage probability setting as input vector $\mathbf{P}_u^{(i,f)}$. To avoid unnecessary computations, when a power coefficient reaches $P_u^{\text{SIC}}(f)$, the updating process for that frequency is not performed anymore. To assure the convergence near to the optimal solution, we halve the value of step size when the updating rule (43) lets the vector unchanged. Hence, the step size updating rule is

$$\mu^{(i)} = \begin{cases} \mu^{(i-1)}/2, & \text{if } \mathbf{P}_u^{(i,F_u)} = \mathbf{P}_u^{(i-1,F_u)} \\ \mu^{(i-1)}, & \text{otherwise.} \end{cases} \quad (44)$$

The algorithm stops when the step size is lower or equal to a certain threshold τ . The overall algorithm is summarized in Algorithm 2.

Taking into account that the objective function of (24) is monotonically non-decreasing, we can prove the following Proposition.

Proposition 4. *If the threshold τ is small enough, Algorithm 2 provides the optimal solution for problem (24).*

Proof. The objective function of problem (24) is a non-decreasing function with gradient

$$\nabla_{\mathbf{P}_u} \sum_{f \in \mathcal{F}_u} P_u(f) = \mathbf{1}. \quad (45)$$

Hence, no saddle point can be found and the optimal solution lay on the border of the feasible set [23, 28]. The power updating rule (43) guarantees that the magnitude of vector \mathbf{P}_u decreases at every iteration, following the minimization direction. Let us suppose that the optimal solution is \mathbf{P}_u^o , and the Algorithm has stopped on point \mathbf{P}_u^* when the threshold is set as t' . If $\mathbf{P}_u^o = \mathbf{P}_u^*$, the proof is completed. Let us now assume that the vector \mathbf{P}_u^* has the same optimal coefficients except for one dimension f , i.e. $P_u^o(f) < P_u^*(f)$, and $P_u^o(g) = P_u^*(g) \forall g \in \mathcal{F}_u \setminus \{f\}$. This means that that exists a feasible point on dimension $f \in \mathcal{F}_u$ that will provide a smaller objective function. Hence, considering $t'' < t'$, using both (44) and (43), it is possible to reduce $P_u^*(f)$ toward $P_u^o(f)$. Reducing t'' , there exists a value of the threshold $0 < t^* \leq t''$ such as updating rules (44) and (43) will provide exactly $P_u^o(f)$. The same results can be extended for the general case where \mathbf{P}_u^o and \mathbf{P}_u^* differ by more than one element, completing the proof. \square

In practice, we can set τ as the minimum variation of power allowed at the BS to obtain the closest to the optimum solution possible.

5 Numerical results

In this section, the performance comparison between OMA and NOMA for spectrum slicing of eMBB and URLLC traffic is presented.

Algorithm 2: Constrained BCD (N-BCD)

```

1 Initialize:  $\mu^{(0)} > 0$ , Compute  $\mathbf{P}_e$  from (19), and  $\mathbf{P}_u^{(0, F_u)}$  using Algorithm 1;  $i \leftarrow 1$ ,  $\mathcal{F}^+ \leftarrow \mathcal{F}_u$ ;
2 while  $\mu^{(i)} > t$  do
3   for  $f \in \mathcal{F}^+$  do
4     Update  $P_u^{(i)}(f)$  using (43);
5     if  $P_u^{(i)}(f) \geq P_u^{SIC}(f)$  then
6        $\mathcal{F}^+ \leftarrow \mathcal{F}^+ \setminus \{f\}$ 
7    $i \leftarrow i + 1$ ;
8   Update  $\mu^{(i)}$  using (44)
9 Output:  $\mathbf{P}_u^* \leftarrow \mathbf{P}_u^{(i-1, F_u)}$ 

```

We consider a resource grid formed by $F = 12$ frequencies and $M = 7$ mini-slots. We consider that the time of a slot is $T = 1$ ms, obtaining $T_m = T/M = 1/7$ ms as the minimum URLLC time-slot of the 5G NR standard [1]. Finally, each mRB has bandwidth $\Delta_f = 180$ kHz.

The reliability requirement of URLLC user is set as $\epsilon_u = 10^{-5}$. The fading channels for both users are Rayleigh distributed with scale parameter $\sqrt{\Gamma_i}$, $i \in \{e, u\}$. In the Monte Carlo simulation used to obtain the look-up table (36), we vary the powers P_i , $i \in \{e, u\}$ of each mRB from -30 dBm to 30 dBm per mRB, with granularity 1 dBm.

For each instance of simulation, we place the users in a cell of 500 m of radius and we compute the power consumption using both OMA and NOMA. The distance d_i , $i \in \{e, u\}$ of the users from the BS is computed inverting the well-known wireless path loss formulation, i.e.

$$d_i = \sqrt[{\alpha}]{10^{G/10} L_i \left(\frac{c}{f_0 4\pi} \right)^2 d_0^{\alpha-2}} \quad (46)$$

where $G = 17.15$ dB is the overall antenna gain of BS and user; $f_0 = 2$ GHz is the central working frequency; c is the speed of light; $d_0 = 10$ m is the free-space region of the cell near to the BS; $\alpha = 4$ is the path loss exponent; $L_i = \sigma^2/\Gamma_i$ is the path loss. We set the receiver noise as $\sigma^2 = -108$ dBm.

In the case of NOMA, we show the results of Algorithms 1 and 2, labeled as N-fea and N-BCD, respectively. For this paradigm, we always present the results obtained setting $F_u = F = 12$. We remark that the choice of this parameter does not influence the eMBB allocation while increasing the number of resources available reduces the power coefficients needed for SIC (see (21) and its comments). We set the threshold of the BCD approach as $\tau = 10^{-7}$. In the case of OMA, we present the results for different frequencies reserved for the URLLC data stream transmission. In particular, we set $F_u \in \{3, 6, 9\}$, labeled as O-3, O-6, O-9, respectively. To correctly compare the performance of schemes with different number of resources available, we fix the number of bits to be transmitted in the whole slot as $N_e = 8640$ and $N_u = \frac{2160}{7}$. In this way, the spectral efficiency for NOMA with $M_u = 1$ are $r_u = 1$ bit/s/Hz and $r_e = 4$ bit/s/Hz. For the other schemes, the spectral efficiencies can be computed through (2).

Firstly, we study the behavior of the power needed for the SIC process given in eq. (21). Fig. 4 shows the overall power spent for the SIC process $P_u^{SIC} = \sum_{f \in \mathcal{F}_u} P_u^{SIC}(f)$ as a function of the distance of the eMBB user d_e . As expected, closer to the BS is the eMBB user, smaller is the power needed for the SIC process. We can also see that the gap between different spectral efficiencies starts to be relevant when $d_e \geq 100$ m. For higher distances, increasing the spectral efficiency increases the value of eMBB power \mathbf{P}_e given by solution (19); for lower distances, the evaluated power is dominated by the terms $1/\gamma_e(f)$. We remark that a low d_e means a high average SNR Γ_e leading to a higher probability of having high instantaneous SNR values $\gamma_e(f)$.

In the following, we show the effect of the URLLC transmission time M_u on the power allocation. Fig. 5 shows the outage probability p_u as a function of the power $P_u(f)$, when all transmitting and interference power coefficient are the same for each mRB, i.e., $P_u(f) = P_u$, $P_e(f) = P_e$, $\forall f \in \mathcal{F}_u$, $\Gamma_u = 30$ dB, and $F_u = 12$. The dashed lines are the outage probability curves with no interference, i.e. $P_e = -\infty$ dBm, while the solid lines represent the outage probability with $P_e = 0$ dBm. We present different plots for different M_u . Increasing the value of M_u , will reduce the spectral efficiency r_u leading to a reduction of the power needed to meet the target outage probability ϵ_u . Therefore, the best solution is design a system able to exploit the

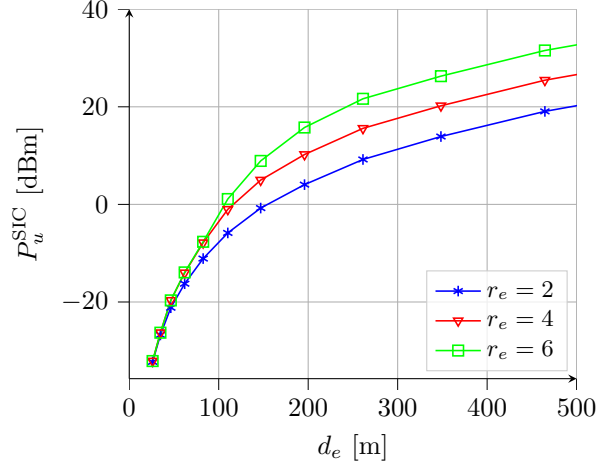


Figure 4: Average power consumption of SIC process as a function of d_e , $F_u = 12$.

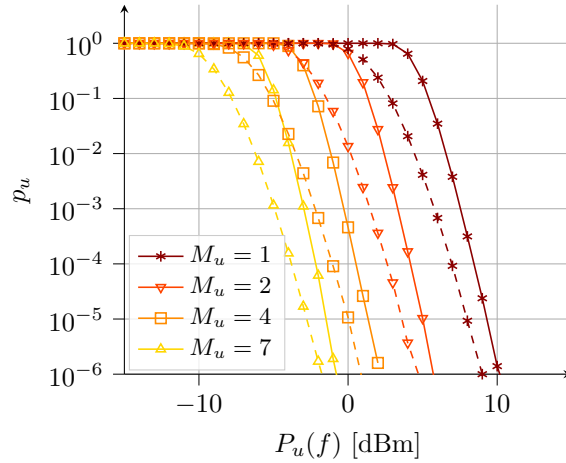
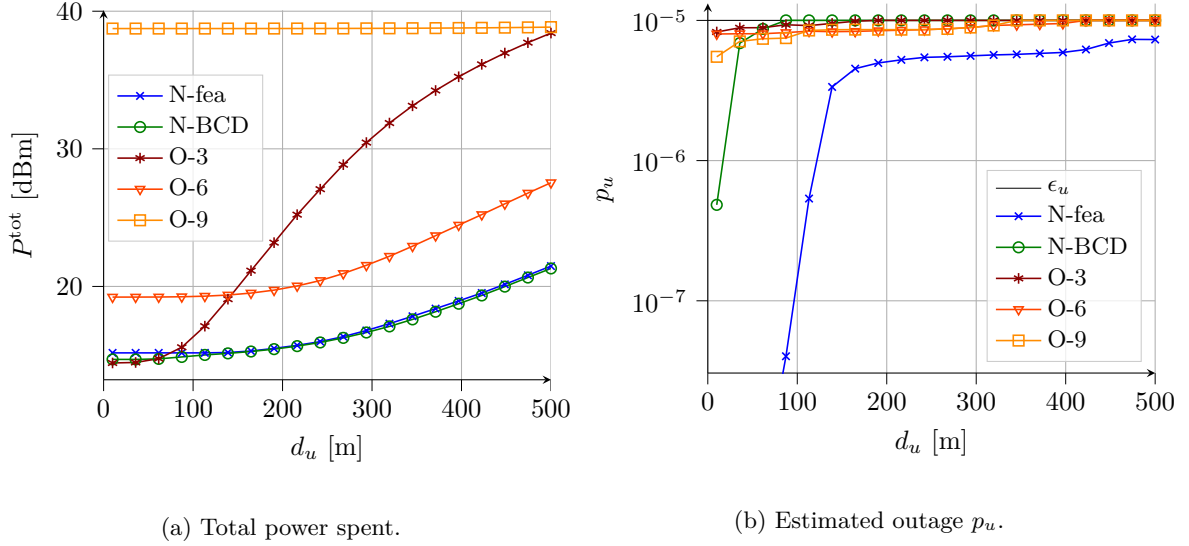
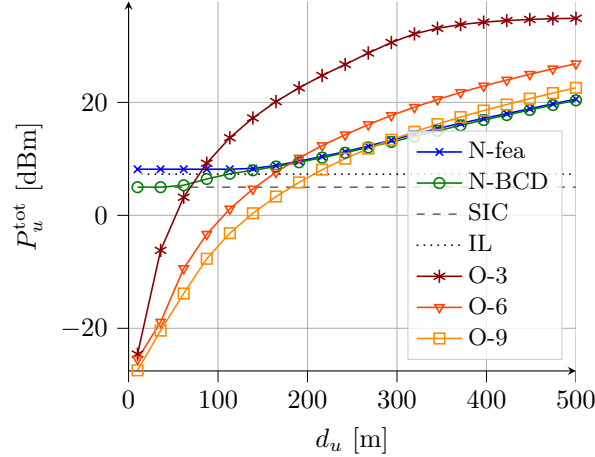


Figure 5: Outage probability p_u versus $P_u(f)$, for $\Gamma_u = 30$ dB, $F_u = 12$ and different M_u . $P_u(f) = P_u$, $P_e(f) = P_e$, $\forall f \in \mathcal{F}_u$. The solid lines are for $P_e(f) = 0$ dBm while dashed lines represent $P_e(f) = -\infty$ dBm, i.e. no interference.

whole latency requirement. Having shown this result, we will focus only on the results of $M_u = 1$ in the remainder of the section, remarking that increasing M_u reduces the overall power spent for all the schemes presented.

Fig. 6a shows the total power spent P^{tot} as a function of d_u , when user e is placed at $d_e = 146.9$ m (corresponding to $\Gamma_e = 50$ dB). We can see that N-fea and N-BCD assure a lower power consumption with respect to the OMA paradigms, as soon as $d_u \geq 75$ m. N-BCD perform better than OMA schemes also for $d_u \geq 65$ dB. The performance gap between N-BCD and N-fea is negligible for every value of d_u under analysis. On the other hand, the OMA paradigm performs slightly better on short distances, i.e., $d_u < 65$ m. In particular, the best results in a high SNR regime are attained by O-3, i.e., giving more mRB to e than to u . Moreover, Fig. 6b presents the corresponding estimated p_u , evaluated with the allocated power coefficients \mathbf{P}_u and \mathbf{P}_e , while the channel gains of u are randomly generated. For the OMA schemes, the target outage is met, guaranteeing $p_u \leq \epsilon_u$. The slight differences from the target outage obtained for short distances are due to the quantization of power available in the tabulate solution, set as 1 dB. The outage probability of N-fea is always lower than ϵ_u , proving that this scheme provides a feasible but not optimal solution. On the other hand, N-BCD reaches exactly the target outage probability until $d_u \geq 85$ m. For shorter distances, the power allocation is dominated by the SIC process limiting the minimum power needed, as we will see in the following.

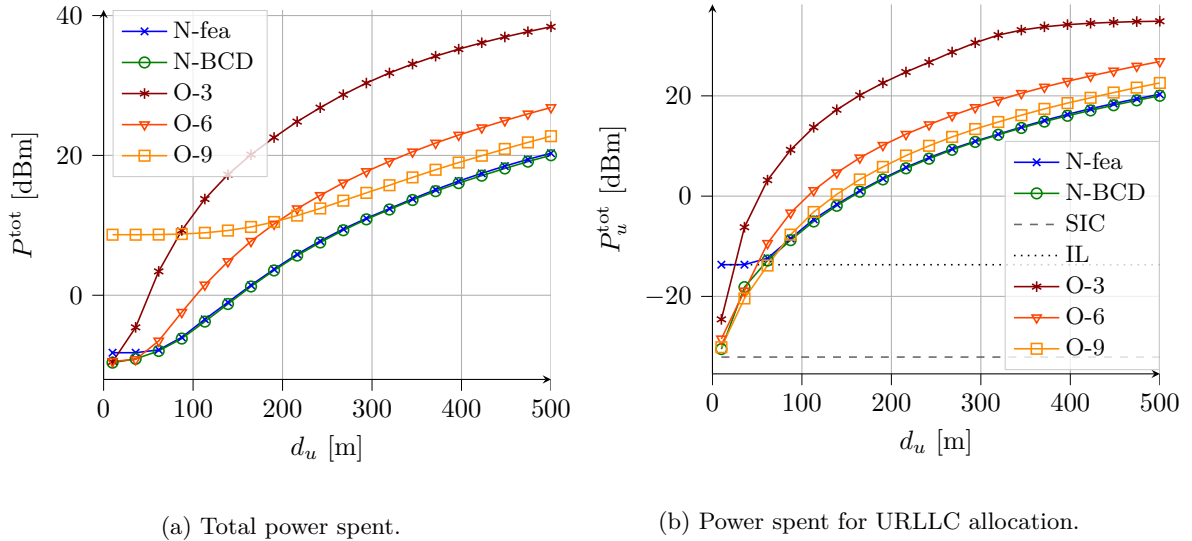
Figure 6: Average results obtained as a function of URLLC distance d_u , $d_e = 146.9$ m.Figure 7: Average URLLC power spent as a function of d_u , $d_e = 146.9$.

To explain the (slight) superiority of OMA to NOMA for small d_u -or high Γ_u regime-, we present the power needed for URLLC and eMBB requirements separately. In Fig. 7, we plot the power spent for the URLLC user $P_u^{\text{tot}} = \sum_{f \in \mathcal{F}_u} P_u(f)$. In this figure, we show the power allocated using the various NOMA and OMA paradigms, as well as the power needed by the SIC process (21), namely SIC, and the power bound of the interference-limited scenario (33), namely IL. It is worth noting that these last two results depend on the eMBB power only. The powers spent for the NOMA schemes are dominated by different effects for short distances. For N-fea, the interference-limited bound is the minimum power achievable. We remark that the power computed by (39) is obtained assuming that all the channels experience the maximum interference. Hence, the mutual information achievable using the power coefficient given by N-fea tends to the approximation (31) on closer distances. On the other hand, N-BCD naturally exploits also the channels with no interference, enabling the possibility of reaching the power needed for the SIC process, which is the lower limit of the NOMA approach. For the OMA schemes, the power spent decreases when resources reserved for the URLLC increase. For short distances, these schemes may consume less power w.r.t. NOMA due to the lack of interference and lower limits. We remark that the frequency diversity gain provided for very short distances ($d_u < 35$ m) is negligible w.r.t. to the gain given by the mean SNR, resulting in comparable performances for the three OMA schemes. Finally, in Table 1, we present the average power spent for the eMBB. Here, the two NOMA schemes are not presented because the eMBB power allocation is the same for both N-fea and N-BCD. From the table, we can infer that the eMBB power plays the dominant role in the

power allocation, explaining why O-9 total power is almost flat on Fig. 6a, even if it can benefit from the lowest URLLC power consumption. The same consideration can be made also for O-6. However, the power spent by O-3 is comparable with the NOMA one. Hence, for $d_e \geq 146.9$, the best allocation scheme between NOMA and O-3 depends only on the URLLC power consumption, clarifying the results obtained in Fig. 6.

Table 1: Average eMBB power spent in dBm.

Γ_e [dB]	d_e [m]	NOMA	O-3	O-6	O-9
30	464.56	33.21	34.18	38.89	58.27
40	261.2	23.36	24.32	29.09	48.54
50	146.9	14.21	14.44	19.23	38.74
60	82.6	5.84	5.84	9.05	28.44
70	46.5	-1.87	-1.87	-0.64	18.79
80	26.1	-9.67	-9.67	-9.67	8.65

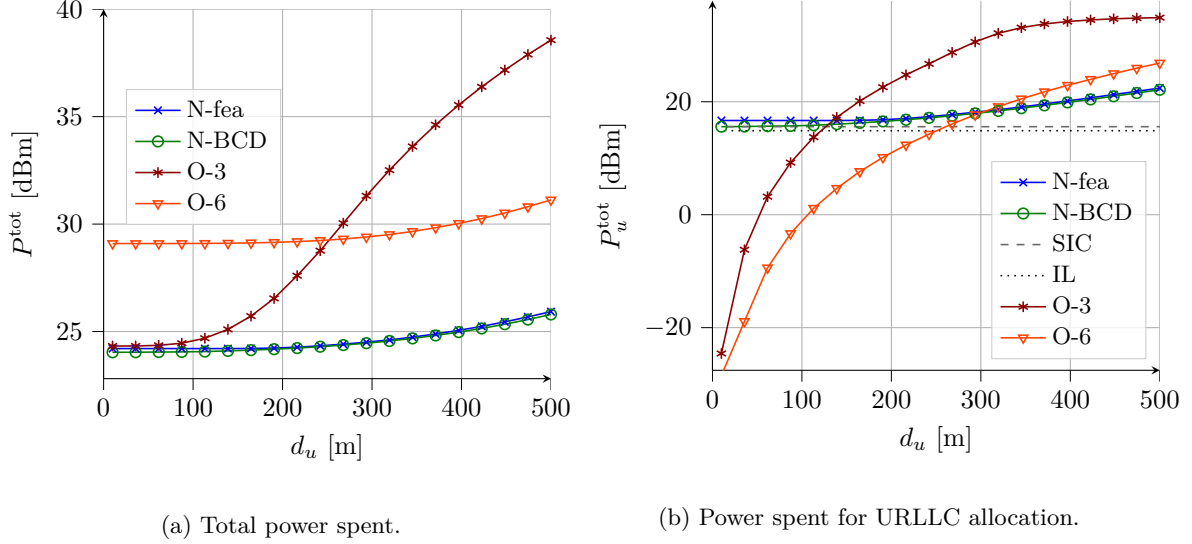
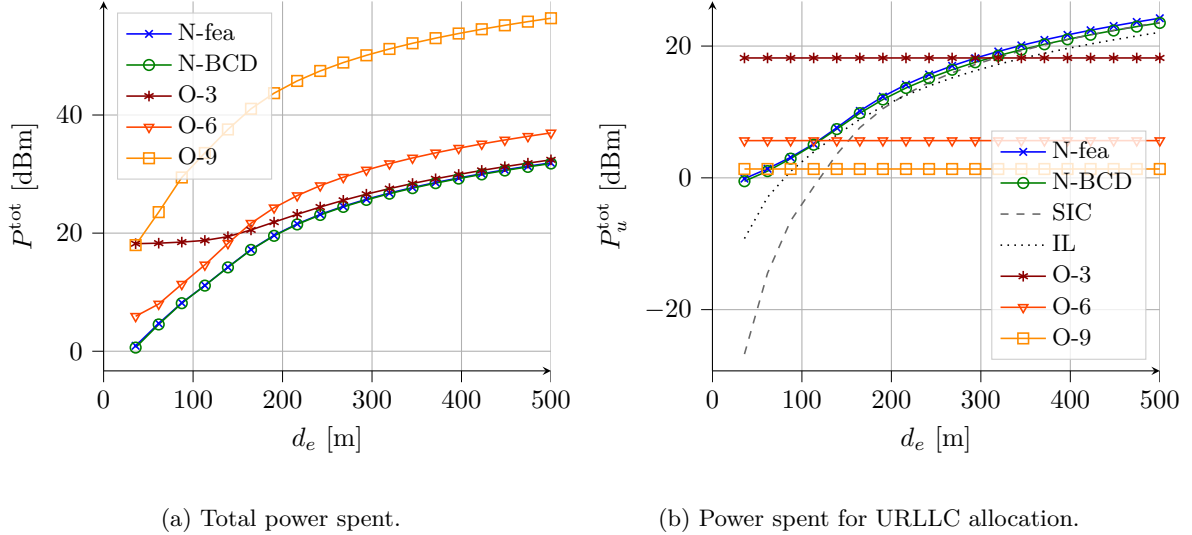
Figure 8: Average results obtained as a function of URLLC distance d_u , $d_e = 26.1$ m.

In Fig. 8, we present the power results in the extreme case of $d_e = 26.1$ m. In this case, the allocated eMBB power is low, and it is the same for NOMA, O-3, and O-6, as shown in Table 1. With this power allocation, the N-BCD approach is never limited by the SIC, and its performances are the best for every value of d_u m. Note that in this extreme case, the best performances between the OMA schemes are attained by O-6, which consume the same eMBB power but benefit from the frequency diversity gain for URLLC allocation.

The last case shown is depicted in Fig. 9, where total and URLLC power consumption are shown when $d_e = 261.2$. In this case, O-9 is not shown because of the enormous power spent for the eMBB allocation (see Table 1). Once again, NOMA schemes outperform OMA schemes. It is interesting to note that SIC bound is greater than the IL bound; the power allocation is dominated by the SIC as soon the URLLC is the user closest to the BS. For this scenario, the simple solution (21) can be employed, guaranteeing the requirements of both users.

Finally, we show in Fig. 10 the power spent as a function of d_e , fixing $d_u = 146.9$ m. In detail, Fig. 10a shows the overall power spent; also in this case the NOMA schemes attain the best performance. Fig. 10a shows the URLLC power spent to meet the reliability requirement. In this case, the OMA power does not change for the different values of d_e , having fixed d_u . On the contrary, NOMA URLLC power is still influenced by the interference given by \mathbf{P}_e , and thus P_u^{tot} increases when d_e increases, accordingly.

We remark that the feasible solution provide by Algorithm 1 is enough to obtain close-to-the-optimal performances for every value of d_e and d_u . Therefore, a practical implementation of the spectrum slicing scheduler can make use of the pre-populated look-up table (36), and still lead to a negligible increase of power consumption w.r.t. the optimal solution.

Figure 9: Average results obtained as a function of URLLC distance d_u , $d_e = 261.2$ m.Figure 10: Average results obtained as a function of eMBB distance d_e , $d_u = 146.9$ m.

6 Conclusions

This paper studied the power and resource allocation for the downlink communication spectrum slicing problem of eMBB and URLLC traffic. We focused on both orthogonal and non-orthogonal multiple access schemes for the parallel channel model. Due to the nature of the communication traffic types, we assumed that the CSI is only statistical for the URLLC, while the eMBB channel relies on instantaneous information. We proposed a feasible and a BCD algorithm able to solve the spectrum slicing problem minimizing the power spent, assuring at the same time the requirements of both kinds of traffic. We also compared the impact of using the aforementioned multiple access scheme for a 5G-like resource grid available. Numerical results showed that the NOMA paradigm attains the best performance in almost all cases. The only exception is for a very close URLLC user, where the frequency diversity gain is negligible. In that case, OMA could attain the best performance depending on the position of the eMBB user. However, the performance gain w.r.t. NOMA is still negligible, proving that NOMA is a promising technology for spectrum slicing. We also proved experimentally that the feasible algorithm provides a close-to-the-optimal power allocation, becoming a possible candidate for a practical resource allocation approach. We believe that this work may be the first

step to understanding the optimal design of a beyond 5G network enabling spectrum slicing on downlink communication.

References

- [1] 3GPP, “Study on New Radio (NR) access technology,” 3rd Generation Partnership Project (3GPP), Technical Report (TR) 38.912, 05 2017, version 14.0.0.
- [2] H. Zhang, N. Liu, X. Chu, K. Long, A. H. Aghvami, and V. C. M. Leung, “Network slicing based 5G and future mobile networks: Mobility, resource management, and challenges,” *IEEE Commun. Mag.*, vol. 55, no. 8, pp. 138–145, 2017.
- [3] S. D’Oro, F. Restuccia, A. Talamonti, and T. Melodia, “The slice is served: Enforcing radio access network slicing in virtualized 5g systems,” in *IEEE INFOCOM 2019 - IEEE Conference on Computer Communications*, 2019, pp. 442–450.
- [4] A. Anand, G. de Veciana, and S. Shakkottai, “Joint scheduling of urllc and embb traffic in 5g wireless networks,” *IEEE/ACM Trans. Netw.*, vol. 28, no. 2, pp. 477–490, 2020.
- [5] M. Elsayed and M. Erol-Kantarci, “AI-Enabled Radio Resource Allocation in 5G for URLLC and eMBB Users,” in *2019 IEEE 2nd 5G World Forum (5GWF)*, 2019, pp. 590–595.
- [6] M. Alsenwi, N. H. Tran, M. Bennis, S. R. Pandey, A. K. Bairagi, and C. S. Hong, “Intelligent resource slicing for eMBB and URLLC coexistence in 5G and beyond: A deep reinforcement learning based approach,” *IEEE Trans. Wireless Commun.*, pp. 1–1, 2021.
- [7] P. Xu, Z. Ding, X. Dai, and H. V. Poor, “NOMA: an information theoretic perspective,” *CoRR*, vol. abs/1504.07751, 2015.
- [8] P. Popovski, K. F. Trillingsgaard, O. Simeone, and G. Durisi, “5G wireless network slicing for eMBB, URLLC, and mMTC: A communication-theoretic view,” *IEEE Access*, vol. 6, pp. 55 765–55 779, 2018.
- [9] A. E. Kalør and P. Popovski, “Ultra-reliable communication for services with heterogeneous latency requirements,” in *2019 IEEE Globecom Workshops (GC Wkshps)*, 2019, pp. 1–6.
- [10] Y. Li, C. Hu, J. Wang, and M. Xu, “Optimization of URLLC and eMBB multiplexing via deep reinforcement learning,” in *2019 IEEE/CIC International Conference on Communications Workshops in China (ICCC Workshops)*, 2019, pp. 245–250.
- [11] F. Chiarioti, I. Leyva-Mayorga, C. Stefanović, A. E. Kalør, and P. Popovski, “Spectrum slicing for multiple access channels with heterogeneous services,” *Entropy*, vol. 23, no. 6, 2021.
- [12] F. Yilmaz and M.-S. Alouini, “Outage capacity of multicarrier systems,” in *2010 17th International Conference on Telecommunications*, 2010, pp. 260–265.
- [13] B. Bai, W. Chen, K. B. Letaief, and Z. Cao, “Outage exponent: A unified performance metric for parallel fading channels,” *IEEE Trans. Inf. Theory*, vol. 59, no. 3, pp. 1657–1677, 2013.
- [14] J. P. Coon, D. E. Simmons, and M. D. Renzo, “Approximating the outage probability of parallel fading channels,” *IEEE Commun. Lett.*, vol. 19, no. 12, pp. 2190–2193, 2015.
- [15] X. Wang, J. Wang, L. He, and J. Song, “Outage analysis for downlink NOMA with statistical channel state information,” *IEEE Wireless Commun. Lett.*, vol. 7, no. 2, pp. 142–145, 2018.
- [16] S. Li, M. Derakhshani, S. Lambotharan, and L. Hanzo, “Outage probability analysis for the multi-carrier NOMA downlink relying on statistical CSI,” *IEEE Trans. Commun.*, vol. 68, no. 6, pp. 3572–3587, 2020.
- [17] C. She, C. Yang, and T. Q. S. Quek, “Radio resource management for Ultra-Reliable and Low-Latency Communications,” *IEEE Commun. Mag.*, vol. 55, no. 6, pp. 72–78, 2017.
- [18] Y. Polyanskiy, H. V. Poor, and S. Verdú, “Channel coding rate in the finite blocklength regime,” *IEEE Trans. Inf. Theory*, vol. 56, no. 5, pp. 2307–2359, 2010.
- [19] W. Yang, G. Durisi, T. Koch, and Y. Polyanskiy, “Quasi-static multiple-antenna fading channels at finite blocklength,” *IEEE Trans. Inf. Theory*, vol. 60, no. 7, pp. 4232–4265, 2014.
- [20] G. Durisi, T. Koch, and P. Popovski, “Toward massive, ultra reliable, and low-latency wireless communication with short packets,” *Proc. IEEE*, vol. 104, no. 9, pp. 1711–1726, 2016.
- [21] D. Tse and P. Viswanath, *Fundamentals of Wireless Communication*. USA: Cambridge University Press, 2005.

- [22] P. He, L. Zhao, S. Zhou, and Z. Niu, "Water-filling: A geometric approach and its application to solve generalized radio resource allocation problems," *IEEE Trans. Wireless Commun.*, vol. 12, no. 7, pp. 3637–3647, 2013.
- [23] L. P. Qian, Y. J. Zhang, and J. Huang, "MAPEL: Achieving global optimality for a non-convex wireless power control problem," *IEEE Trans. Wireless Commun.*, vol. 8, no. 3, pp. 1553–1563, 2009.
- [24] M. Jaggi, "Revisiting frank-wolfe: Projection-free sparse convex optimization," in *Proceedings of the 30th International Conference on International Conference on Machine Learning - Volume 28*, ser. ICML'13. JMLR.org, 2013, p. I–427–I–435.
- [25] D. Palomar and J. Fonollosa, "Practical algorithms for a family of waterfilling solutions," *IEEE Transactions on Signal Processing*, vol. 53, no. 2, pp. 686–695, 2005.
- [26] H.-J. M. Shi, S. Tu, Y. Xu, and W. Yin, "A primer on coordinate descent algorithms," *arXiv: Optimization and Control*, 2017.
- [27] Y. Xu and W. Yin, "A globally convergent algorithm for nonconvex optimization based on block coordinate update," *J Sci Comput*, vol. 72, no. 2, pp. 700–734, 2017.
- [28] S. Boyd and L. Vandenberghe, *Convex Optimization*. Cambridge University Press, 2004.